

Gamow-Teller transitions studied in the high-resolution  $^{64}\text{Ni}(^3\text{He}, t)^{64}\text{Cu}$  reaction

L. Popescu,<sup>1,\*</sup> T. Adachi,<sup>2</sup> G. P. A. Berg,<sup>3,†</sup> P. von Brentano,<sup>4</sup> D. Frekers,<sup>5</sup> D. De Frenne,<sup>1</sup> K. Fujita,<sup>6</sup> Y. Fujita,<sup>2</sup> E.-W. Grewe,<sup>5</sup> M. N. Harakeh,<sup>3</sup> K. Hatanaka,<sup>6</sup> E. Jacobs,<sup>1</sup> K. Nakanishi,<sup>6</sup> A. Negret,<sup>1,‡</sup> Y. Sakemi,<sup>6</sup> Y. Shimbara,<sup>6</sup> Y. Shimizu,<sup>6</sup> Y. Tameshige,<sup>2</sup> A. Tamii,<sup>6</sup> M. Uchida,<sup>7</sup> H. J. Wörtche,<sup>3</sup> and M. Yosoi<sup>7</sup>

<sup>1</sup>Vakgroep Subatomaire en Stralingsfysica, Universiteit Gent, B-9000 Gent, Belgium

<sup>2</sup>Department of Physics, Osaka University, Toyonaka, Osaka 560-0043, Japan

<sup>3</sup>KVI, University of Groningen, NL-9747 AA Groningen, The Netherlands

<sup>4</sup>IKP Köln University, Köln, Germany

<sup>5</sup>Institut für Kernphysik, Westfälische Wilhelms-Universität Münster, D-48149 Münster, Germany

<sup>6</sup>RCNP, Osaka University, Ibaraki, Osaka 567-0047, Japan

<sup>7</sup>Department of Physics, Kyoto University, Sakyo, Kyoto 606-8224, Japan

(Received 27 April 2009; published 12 June 2009)

To study the Gamow-Teller (GT) transitions to the  $pf$ -shell nucleus  $^{64}\text{Cu}$ , the  $^{64}\text{Ni}(^3\text{He}, t)^{64}\text{Cu}$  experiment was performed at the Research Center for Nuclear Physics (RCNP) Ring Cyclotron, Osaka, using a  $^3\text{He}$  beam of 140 MeV/nucleon. The outgoing tritons were momentum analyzed by the Grand Raiden spectrometer at  $0^\circ$ . A high energy resolution of 32 keV (full width at half-maximum) allowed the separation of individual levels in the excitation-energy region from 0 to 3.5 MeV. In addition to the ground state (gs), known to be a  $J^\pi = 1^+$  GT state, many low-lying states showed  $L = 0$  nature, suggesting that they are candidates for GT states. Because the GT strength  $B(\text{GT})$  for the gs transition is known from the  $\beta$ -decay measurement, the strengths for the excited states could be determined using the proportionality between the  $B(\text{GT})$  and the reaction cross section extrapolated to  $q = 0$  momentum transfer. At higher excitation energies, the level density becomes high and the so-called GT giant resonance dominates the spectrum. The lower and the upper limits of the strength contained in this energy region were estimated. Our results show that less than 55% of the strength predicted by the Ikeda sum rule is located in the excitation-energy region from 0 to 17 MeV.

DOI: 10.1103/PhysRevC.79.064312

PACS number(s): 25.55.Kr, 21.10.Hw, 24.30.Gd, 27.50.+e

## I. INTRODUCTION

The  $^{64}\text{Ni}(^3\text{He}, t)^{64}\text{Cu}$  reaction was used to investigate the distribution of Gamow-Teller (GT) strengths  $B(\text{GT}^-)$  starting from the ground state (gs) of  $^{64}\text{Ni}$  in the  $\beta^-$  direction. There were several motivations for this study:

- (i) Given the direct calibration from  $\beta$ -decay measurements [1], we have the possibility to determine the unit cross section [see Eq. (2)] experimentally and use it as standard for  $pf$ -shell nuclei [2].
- (ii) Considering the  $B(\text{GT}^+)$  strength obtained in the  $^{64}\text{Ni}(d, ^2\text{He})^{64}\text{Co}$  experiment [3], we can study the quenching of the GT strength [4].
- (iii) By combining the  $B(\text{GT}^-)$  distribution with the  $B(\text{GT}^+)$  distribution that can be obtained in the study of the  $^{64}\text{Zn}(d, ^2\text{He})^{64}\text{Cu}$  reaction, we can deduce the nuclear matrix element of the two-neutrino double- $\beta$  decay ( $2\nu 2\beta$ ) from the gs of  $^{64}\text{Zn}$  to the gs of  $^{64}\text{Ni}$  [5].
- (iv) Our results supplement the data base needed to calibrate theoretical models [5–8].

The  $\beta$ -decay studies supply the most direct information about the  $B(\text{GT})$ , but the accessible range of excitation energy

$E_x$  is limited by a small  $Q$  value. In the  $\beta$ -decay study of  $^{64}\text{Cu}$ , the  $B(\text{GT})$  value was obtained only for the gs transition. Charge-exchange (CE) reactions, like the  $(p, n)$  reaction, can access analogous GT transitions without the  $Q$ -value limitation. In particular, the CE reactions performed at angles around  $0^\circ$  and intermediate energies ( $E \geq 100$  MeV/nucleon) were shown to be good probes of GT transition strengths due to the close proportionality between the cross sections at  $0^\circ$  extrapolated to  $q = 0$  transfer and the  $B(\text{GT})$  values [2],

$$\frac{d\sigma^{\text{CE}}}{d\Omega}(q=0) \simeq K^{\text{CE}} N_{\sigma\tau}^{\text{CE}} |J_{\sigma\tau}(0)|^2 B(\text{GT}) \quad (1)$$

$$= \widehat{\sigma}_{\text{GT}}(q=0) B(\text{GT}), \quad (2)$$

where  $J_{\sigma\tau}(0)$  is the volume integral of the effective interaction  $V_{\sigma\tau}$  at  $q = 0$  momentum transfer,  $K^{\text{CE}}$  the kinematic factor for the CE reaction,  $N_{\sigma\tau}^{\text{CE}}$  the distortion factor, and  $\widehat{\sigma}_{\text{GT}}(q=0)$  the unit cross section for the GT transition at  $q = 0$ .

In the last decade, precise beam-matching techniques were applied to the  $(p, n)$ -type  $(^3\text{He}, t)$  reaction measured at  $0^\circ$  and at intermediate incident energies. A good energy resolution  $\Delta E = 30$  keV [full width at half-maximum (fwhm)] was realized [9,10]. Therefore, it was expected that states unresolved in earlier  $(p, n)$  measurements [11] could now be clearly resolved. The validity of the close proportionality in  $(^3\text{He}, t)$  reactions at 140 MeV/nucleon between cross sections extrapolated to  $q = 0$  and GT transition rates has been demonstrated for transitions with  $\Delta L = 0$  nature and for values of  $B(\text{GT}) \geq 0.04$  by studying analogous GT transitions in the  $A = 27$  mirror nuclei,  $^{27}\text{Al}$  and  $^{27}\text{Si}$  [12], and the

\*Permanent address: SCK•CEN, B-2400 Mol, Belgium.

†Permanent address: Department of Physics, University of Notre Dame, 225 Nieuwland Science Hall, Notre Dame, IN 46446-5670, USA.

‡Permanent address: NIPNE, Bucharest, Romania.

$A = 26$  nuclei,  $^{26}\text{Mg}$ ,  $^{26}\text{Al}$ , and  $^{26}\text{Si}$  [13]. An exception is also discussed in Ref. [14].

## II. EXPERIMENT

We performed the  $^{64}\text{Ni}(^3\text{He}, t)^{64}\text{Cu}$  experiment at the high energy resolution facility of the Research Center for Nuclear Physics (RCNP), Osaka. The “WS-course” [15] was used in combination with the Grand Raiden spectrometer [16], which was set at  $0^\circ$  with respect to the beam axis. The  $^3\text{He}$  beam was accelerated to 140 MeV/nucleon by the  $K = 400$  Ring Cyclotron [17]. A self-supporting foil of  $^{64}\text{Ni}$  with an isotopic purity of 97.92% and thickness of  $0.473\text{ mg/cm}^2$  was used as a target. The outgoing tritons were momentum analyzed within the full acceptance of the spectrometer and detected with a focal-plane detector system allowing for particle identification and track reconstruction in horizontal and vertical directions [18]. Good angular resolution of  $\leq 5$  mrad (fwhm) was achieved by applying the angular dispersion-matching technique [19] and the “overfocus mode” of the spectrometer [20]. In the data analysis, the acceptance of the spectrometer was subdivided in scattering-angle regions using the track information.

The main contaminants in the target were  $^{58}\text{Ni}$  (0.92%),  $^{60}\text{Ni}$  (0.73%), and  $^{62}\text{Ni}$  (0.38%). Given the small admixtures of the contaminants, they are not expected to contribute significantly to the  $^{64}\text{Cu}$  spectrum. Moreover, the comparatively small negative  $Q$  value of the  $^{64}\text{Ni}(^3\text{He}, t)$  reaction essentially makes the low energy levels of  $^{64}\text{Cu}$  free from contributions of the contaminants. The  $(^3\text{He}, t)$  reaction on  $^{60}\text{Ni}$  and  $^{62}\text{Ni}$  was measured under the same experimental conditions. Also, a  $^{58}\text{Cu}$  spectrum obtained in the  $^{58}\text{Ni}(^3\text{He}, t)$  reaction is given in Ref. [21]. The strongest peaks in the  $^{62}\text{Cu}$ ,  $^{60}\text{Cu}$ , and  $^{58}\text{Cu}$  spectra are located at 4.61, 2.54, and 1.05 MeV, respectively, which correspond to 6.88, 6.99, and 7.94 MeV in the  $^{64}\text{Cu}$  spectrum. None of these peaks contributes significantly to the spectrum shown in Fig. 1.

In the present measurement, an energy resolution of 32 keV (fwhm) was achieved. Separated peaks were observed up to  $E_x \sim 6$  MeV in the “ $0^\circ$  spectrum” (see Fig. 1). Because the proton and neutron separation energies are 7.20 and 7.92 MeV,

respectively, no broadening of the transitions is expected in this excitation-energy region.

## III. DATA ANALYSIS

The intensities of individual peaks were obtained by employing a peak-decomposition program using the peak shape deduced from the 0.0, 0.926, and 1.296 MeV peaks as references. The excitation energies ( $E_x$ ) of the peaks are given in Table I. All of the prominent states in the low excitation-energy region that are listed in Ref. [1] could be identified. The excitation energies are in agreement with the values of Ref. [1] within 10 keV. For details of our energy calibration, see Ref. [22].

The yields of the transitions were compared for the spectra with angle cuts  $\theta = 0^\circ\text{--}0.3^\circ$ ,  $0.5^\circ\text{--}1^\circ$ ,  $1.0^\circ\text{--}1.5^\circ$ ,  $1.5^\circ\text{--}2.0^\circ$ . All those transitions that exhibit a relative decrease in strength similar to that of the known  $\Delta L = 0$  gs transition were considered candidates for GT states. The Fermi strength is expected to be concentrated exclusively in the transition to the isobaric analog state (IAS) located at 6.82 MeV. As an example, Fig. 2 shows the relative cross-section ratios for peaks in the excitation-energy region  $0 \leq E_x \leq 2.5$  MeV normalized to the gs value. The peaks for which all three ratios are close to one correspond to the accepted GT peaks.

To derive  $B(\text{GT})$  values from Eq. (2), a standard  $B(\text{GT})$  value from a  $\beta$ -decay measurement is needed. The gs transition from the  $\beta$  decay of  $^{64}\text{Cu}$  was used for this purpose and the value  $B(\text{GT}^-) = 0.123 \pm 0.002$  was calculated following Ref. [23]. This value differs slightly from that given in Ref. [23], because we now use a more recent  $\log ft$  value of  $4.971 \pm 0.004$  for the  $\text{EC}/\beta^+$ -decay of  $^{64}\text{Cu}$  (gs) to  $^{64}\text{Ni}$  (gs) [1]. Also, a recent coupling constant ratio  $g_A/g_V = -1.266 \pm 0.004$  [24] was used. Our unit system gives a value of  $B(\text{GT}) = 3$  for the  $\beta$  decay of the free neutron. The  $B(\text{GT}^-)$  values for the excited states were calculated from their peak intensities corrected for the dependence on the excitation energy and assuming the proportionality of Eq. (2). The correction was made using the results of distorted-wave Born approximation (DWBA) calculations (for details, see Ref. [22]). This correction was less than 6% for  $E_x \leq 7$  MeV.

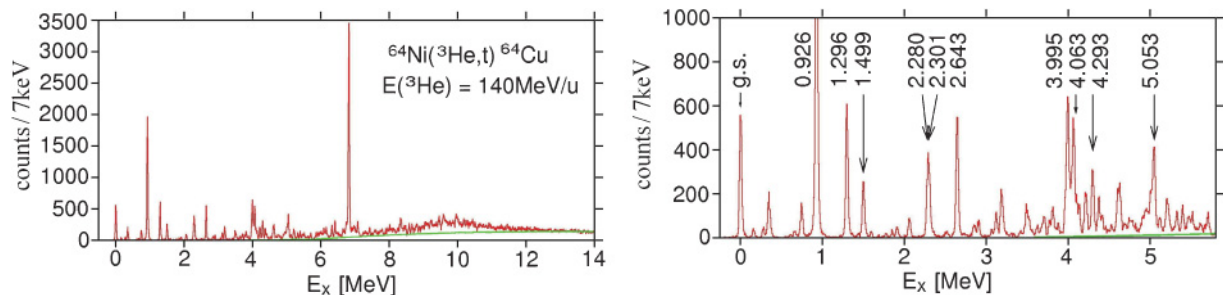


FIG. 1. (Color online) The  $^{64}\text{Cu}$  spectrum for scattering angles between  $0^\circ$  and  $0.3^\circ$ . For a better observation, the low energy region is expanded in the right part of the figure. Several  $J^\pi = 1^+$  states are indicated by their excitation energies given in MeV. The most intense peak in the spectrum, appearing at 6.82 MeV, is the isobaric analog state of  $^{64}\text{Ni}$  ( $J^\pi = 0^+$ ). The continuum background is drawn as a smooth line (see text for details).

TABLE I. Excitation energies and  $B(\text{GT}^-)$  values for transitions to  $J^\pi = 1^+$  states in  $^{64}\text{Cu}$  for  $E_x \leq 3.5$  MeV.

Evaluated values <sup>a</sup>		Present experiment		
$E_x$ (MeV)	$J^\pi$	$E_x$ (MeV)	$\Delta L$	$B(\text{GT}^-)$
0.0	$1^+$	0.0	0	0.123(2) <sup>b</sup>
0.159	$2^+$	0.159	$\geq 1$	
0.278	$2^+$	0.277	$\geq 1$	
0.344	$1^+$	0.344	0	0.037(3)
0.362	$3^+$	0.365	$\geq 1$	
0.609	$2^+$	0.606	$\geq 1$	
0.663	$1^+$	0.663	0	0.006(1)
0.739	$2^+$	??	??	
0.746	$(3)^+$	0.745	$\geq 1$	
0.927	$(1)^+$	0.926	0	0.426(13)
1.298	$(1^+)$	1.296	0	0.129(5)
1.354	$(3)^+$	1.357		
1.439	$(1)^+$	1.435		
1.499	$(2)^-$	1.499	0	0.059(3)
1.594	$(1^+, 2)$	1.591		
1.683	$\leq 3$	1.683	$\geq 1$	
1.779	$(1^+, 2^+)$	1.775		
1.853	$(1^+, 2^+)$	1.850		
1.905	$(1^+, 2)$	1.911	1	
1.918	$\leq 4$			
2.021	$(1^+, 2^+, 3^+)$			
2.060	$\leq 3$	2.061		c
2.065	$\leq 4$			
2.280	$\leq 3$	2.280 } 2.301 } 2.350 }	0	0.114(4)
2.301	$\leq 3$			
2.355	$\leq 3$			
2.381	-			
2.465	$(1^-, 2^-)$	2.470	$\geq 1$	
2.507	$(\leq 3)$	2.511	$\geq 1$	
2.648	$\leq 3$	2.643	0	0.125(4)
2.718	$(1^-, 2^-)$	2.723	$\geq 1$	
2.764	$(1^-, 2^-)$	2.760	$\geq 1$	
2.830 <sup>d</sup>	$\leq 3$	2.821	$\geq 1$	
2.854	$(0^+ \text{ to } 3^+)$	2.854	0	0.014(1)
2.897	$(1^+)$	2.905	0	0.017(1)
2.985	$(1^-, 2^-)$	2.981	$\geq 1$	
3.034	$(0^-, 1^-, 2^-)$	3.024	$\geq 1$	
3.072	$(2^-, 3^-, 4^-)$	3.064		
3.125	$(\leq 3)$	3.122		
3.191	$(\leq 4)$	3.185		
3.208	$(0, 1, 2)$	3.207		
3.258	$(0, 1, 2)$	3.252		
3.313	$(0, 1, 2)$	3.303	$\geq 1$	
3.344	$(\leq 3)$	3.339		

<sup>a</sup>From Ref. [1].

<sup>b</sup>Calculated using the  $\log ft$  value from Ref. [1].

<sup>c</sup> $B(\text{GT}^-) = 0.021(1)$  if this is a GT peak.

<sup>d</sup>2.823 MeV in other studies [1].

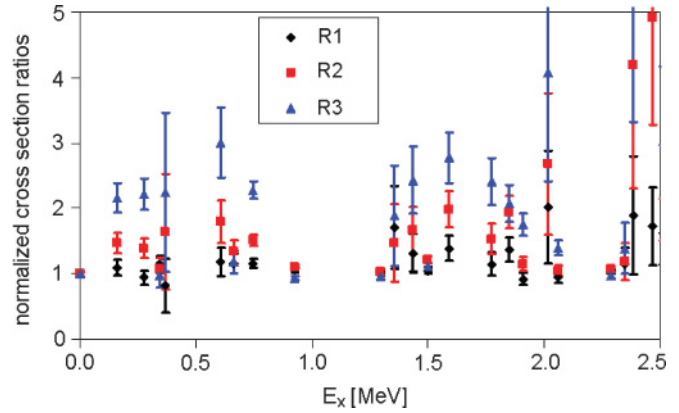


FIG. 2. (Color online) Angular distributions for peaks in  $^{64}\text{Cu}$  spectrum as ratios of relative cross sections:  $R1 = \sigma(0.5^\circ-1.0^\circ)/\sigma(0^\circ-0.3^\circ)$ ,  $R2 = \sigma(1.0^\circ-1.5^\circ)/\sigma(0^\circ-0.3^\circ)$ ,  $R3 = \sigma(1.5^\circ-2.0^\circ)/\sigma(0^\circ-0.3^\circ)$ , normalized to the gs peak. The peaks for which all three ratios are close to one correspond to the accepted GT peaks.

The obtained  $B(\text{GT}^-)$  values for individual transitions in the excitation-energy region  $0 \leq E_x \leq 3.5$  MeV are given in Table I. The uncertainty in the determined excitation energies is estimated to be  $\Delta E_x = 10$  keV. The indicated uncertainty in the obtained  $B(\text{GT}^-)$  values represents only the statistical uncertainty. In addition, 5% uncertainties are induced by the extrapolation to  $q = 0$  and 13% by the uncertainty in the determined value for the unit cross section. This leads to a systematic uncertainty of 14% that has to be considered on top of the uncertainties given in Table I. The large uncertainty in the unit cross section is due to the rather weak gs transition, which has been used to derive the unit cross section.

Our energy resolution was not sufficient to separate the levels at 2.280 and 2.301 MeV. As the cross section of the doublet showed a clear  $\Delta L = 0$  angular distribution (see Fig. 2), we determined the  $B(\text{GT}^-)$  for the doublet and not for the two components separately. Considerable uncertainties induced by the peak fitting are avoided in this way.

Another aspect to be mentioned for this low energy region is the nature of the levels at 1.435 and 1.499 MeV. The spins and parities of these levels reported in Ref. [1] are  $(1)^+$  and  $(2)^-$ , respectively. The present analysis does not confirm this. The transition at 1.435 MeV is weak and the large statistical error on its cross section doesn't allow an accurate angular distribution analysis. However, the peak appearing at 1.499 MeV in the  $^{64}\text{Cu}$  spectrum shows a clear  $\Delta L = 0$  angular distribution of the cross section suggesting a  $J^\pi = 1^+$  for this level (see Fig. 2).

Because of the low intensity of several transitions, their multipolarity could not be determined. The corresponding levels are indicated in Table I by their excitation energy.

In the excitation-energy region  $3.5 \leq E_x \leq 7.2$  MeV a small amount of physical background is observed in the spectrum. This background was assumed as a smooth line connecting the minima between the peaks, as shown in Fig. 1. Because we are interested in the discrete levels in this region, we obtained the counts of peaks after subtracting this physical-background part. The differences in the  $B(\text{GT}^-)$  values were insignificant

for the peaks located below  $E_x = 5.8$  MeV. The analysis of the higher excitation-energy region (see below) indicates that the physical-background part in the region  $3.5 \leq E_x \leq 7.2$  MeV of the  $0^\circ$  spectrum represents the tail of the Gamow-Teller Giant Resonance (GTGR).

Even the high energy resolution achieved in this experiment often became insufficient to separate individual levels. Broad peaks containing contributions from several levels were present and their decomposition was not always obvious. Six peaks around 4 MeV are grouped in a bump that shows a  $\Delta L = 0$  character. Due to the limited experimental data, a multipole decomposition analysis could not be performed. Therefore, in the analysis, we assumed no contributions from higher order multipoles and calculated the  $B(\text{GT}^-)$  value for the entire group. The  $B(\text{GT}^-)$  for the broad peaks around 5, 6, and 6.5 MeV was extracted in a similar way.

The obtained results are given in Table II. A systematic uncertainty of 24% should be considered in addition to the uncertainties of the  $B(\text{GT}^-)$  values given in Table II. This uncertainty includes contributions from the error in the calculated value for the unit cross section, uncertainties in the extrapolation to  $q = 0$ , and uncertainties related to the assumptions that we made for the contributions of higher order multipoles. The uncertainty in the determined excitation energies is  $\Delta E_x = 15$  keV.

In the  $E_x \geq 7.2$  MeV region, the level density became even higher. Although several fine structures could be found (see Fig. 4), it was not possible to analyze the spectrum into separated levels.

The continuum from quasifree scattering (QFS) [26] is expected above the proton separation energy of  $S_p = 7.20$  MeV. Because there is no established theory for reliably calculating the cross section of the QFS continuum, a background described by a smooth line was subtracted in the analysis (see Fig. 3). By removing this continuum part and considering that the remaining structure part can be attributed entirely to the GTGR, the value  $B(\text{GTGR}^-) = 8.4$

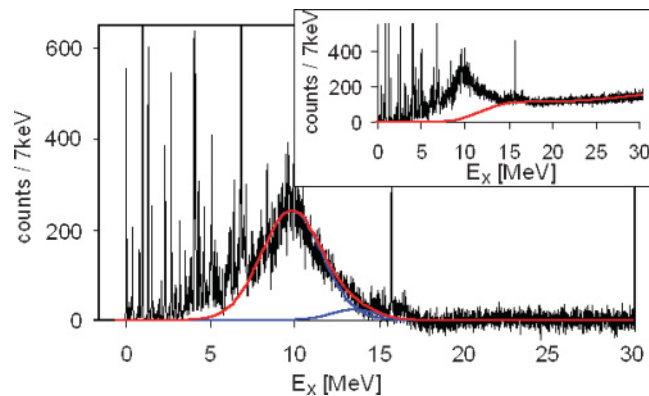


FIG. 3. (Color online) Fit of the  $^{64}\text{Cu}$  spectrum in the GTGR energy region after subtracting the contributions from QFS. The estimation of these contributions is shown by the red curve in the insert. This figure presents the spectrum for scattering angles between  $0^\circ$  and  $0.3^\circ$ . The peak above 15 MeV corresponds to the gs to gs transition in the  $^{12}\text{C}(^3\text{He}, t)^{12}\text{N}$  reaction and it is caused by a small contamination of the target with  $^{12}\text{C}$ .

TABLE II. Excitation energies of GT transition candidates in  $^{64}\text{Cu}$  and the obtained  $B(\text{GT}^-)$  values for the excitation-energy region  $3.4 \leq E_x \leq 6.8$  MeV.

Evaluated values <sup>a</sup>		Present experiment		
$E_x$ (MeV)	$J^\pi$	$E_x$ (MeV)	$\Delta L$	$B(\text{GT}^-)$
3.525	( $\leq 4$ )	3.522	0	0.016(1)
3.686		3.674	0	0.032(1)
3.712	( $\leq 3$ )	3.705		
3.803	( $\leq 3$ )	3.804	0	0.033(1)
3.827	( $1^+, 2, 3$ )	3.827		
		3.966	0	0.054(2)
		3.995		
3.991	(1-4)	4.031	0	0.373(11)
4.034	(0, 1, 2)	4.063		
4.072		4.101		
		4.136		
		4.205	0	0.077(3)
		4.222		
4.328	( $1^+, 2, 3^-$ )	4.293	0	0.065(2)
		4.311		
		4.373	0	0.085(3)
		4.313		
		4.452		
		4.599	0	0.016(1)
		4.630		
		4.744	0	0.331(6)
5.000	( $0-4^-$ )	4.877		
		4.916		
		4.957		
		5.000		
		5.030		
		5.053	0	0.055(2)
		5.116		
		5.198	0	0.025(2)
		5.227		
		5.322	0	0.030(2)
		5.397		
		5.513	0	0.021(2)
		5.569		
		5.617	0	0.021(1)
		5.665		
		5.665	0	0.030(1)
		5.705		

TABLE II. (Continued.)

Evaluated values <sup>a</sup>		Present experiment		
$E_x$ (MeV)	$J^\pi$	$E_x$ (MeV)	$\Delta L$	$B(\text{GT}^-)$
		5.809	0	0.220(6)
		5.864		
		5.922		
		5.967		
		6.003		
		6.116		
		6.156		
		6.201		
		6.321	0	0.044(2)
		6.413	0	0.065(3)
		6.464	0	0.045(2)
		4.493		
		6.529		
		6.570		
		6.740	0	0.048(4)
6.810	(0 <sup>+</sup> )	6.809	0	b
6.826	(0 <sup>+</sup> )	6.825		

<sup>a</sup>From Ref. [1].

<sup>b</sup>IAS of <sup>64</sup>Ni gs [1,25].

was obtained. The best fit of the GTGR was obtained by summing two Gaussian functions.

Figure 4 shows the fit of the GTGR region if no QFS continuum contributions are considered. Under this assumption, the value  $B(\text{GTGR}^-) = 11.2$  is obtained.

#### IV. DISCUSSION

Our experimental results can be divided into three groups, according to the accuracy of the obtained  $B(\text{GT}^-)$  values.

- (i) In the energy region  $0 \leq E_x \leq 3.5$  MeV of the spectrum, the 32 keV energy resolution made the separation

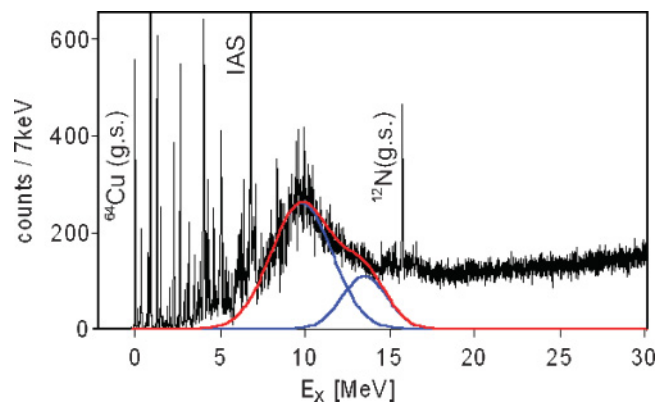


FIG. 4. (Color online) Fit of the <sup>64</sup>Cu spectrum in the GTGR energy region. Contributions from QFS were not considered. This figure presents the spectrum for scattering angles between 0° and 0.3°.

of individual peaks possible. Therefore, the obtained  $B(\text{GT}^-)$  values are given with good accuracy. The total strength found in this region amounts to  $B(\text{GT}^-) = 1.05 \pm 0.02^{\text{stat}} \pm 0.15^{\text{syst}}$ , where the statistical uncertainties have been added in quadrature.

- (ii) Because of the high level density and the insufficient energy resolution, and also because of the ambiguity in assuming the background contributions, the results in the region  $3.5 \leq E_x \leq 7.2$  MeV are less precise. The total strength found in this region amounts to  $B(\text{GT}^-) = 1.59 \pm 0.02^{\text{stat}} \pm 0.38^{\text{syst}}$ .
- (iii) Finally, the third group deals with the high excitation-energy region, dominated by a bump-like structure. An accurate multipole decomposition analysis could not be performed because of the limited data on the angular distribution. If we assume the continuum as shown in the insert of Fig. 3 and consider that the remaining structure part can be attributed entirely to the GTGR, a  $B(\text{GTGR}^-)$  value of 8.4 is obtained. By including also the continuum part (Fig. 4), we obtain the upper limit  $B(\text{GTGR}^-) = 11.2$ .

However, apart from QFS contributions [26], contributions from higher multipole strengths are also expected at these energies, as shown for the case of <sup>90</sup>Zr [27]. Therefore, the total  $B(\text{GT}^-)$  below  $E_x = 17$  MeV can be even less than 11.0 and in any case not larger than 13.8.

According to the Ikeda sum rule, we get  $\sum B(\text{GT}^-) = 3(N - Z) + \sum B(\text{GT}^+)$ . The lower limit of  $\sum B(\text{GT}^+) \approx 1.2$  was determined recently by using the <sup>64</sup>Ni(*d*, <sup>2</sup>He) reaction [3]. Because  $3(N - Z) = 24$ , this implies that the  $\sum B(\text{GT}^-)$  should be larger than 25.2. Our result shows that the total sum of the  $B(\text{GT}^-)$  located in the energy region from 0 to 17 MeV is around 44% and in any case not larger than 55% of the sum-rule-limit value.

In Ref. [28] we investigate the nuclear matrix element of the  $2\nu 2\beta$  decay of nucleus <sup>64</sup>Zn to nucleus <sup>64</sup>Ni by combining the results of this <sup>64</sup>Ni(<sup>3</sup>He, *t*)<sup>64</sup>Cu experiment with the results of the <sup>64</sup>Zn(*d*, <sup>2</sup>He)<sup>64</sup>Cu experiment. The  $2\nu 2\beta$  decay is believed to proceed as a combination of two consecutive virtual single- $\beta$  transitions: from the gs of the mother nucleus <sup>64</sup>Zn to 1<sup>+</sup> states in the intermediate nucleus <sup>64</sup>Cu, which further decay to the gs of the grand daughter nucleus <sup>64</sup>Ni. The obtained  $B(\text{GT}^+)$  and  $B(\text{GT}^-)$  distributions are important also in describing different astrophysical processes [8]. They determine the electron-capture and  $\beta^-$ -decay rates on nuclei, and therefore, the dynamics of the core collapse in a type II supernova [29]. The transition rates in *pf*-shell nuclei are usually calculated within the nuclear shell model. However, these calculations are in severe need of calibration by experimental data. Therefore, the detailed GT strength distribution obtained in our study provides a valuable experimental input for testing various residual *pf*-shell interactions. Comparisons between our results and theoretical calculations are shown and discussed in Ref. [28].

#### V. CONCLUSION

We measured the  $\text{GT}^-$  strength distribution in the <sup>64</sup>Ni(<sup>3</sup>He, *t*)<sup>64</sup>Cu reaction at an intermediate incident energy

of 140 MeV/nucleon. Given the calibration from the  $\beta$ -decay measurements [1], we determined the unit cross section experimentally. This value is used as standard for  $pf$ -shell nuclei [30].

The achieved energy resolution ( $\Delta E = 32$  keV) allowed a good separation of peaks corresponding to individual levels in the low energy region of the spectrum  $0 \leq E_x \leq 3.5$  MeV, where the  $B(GT^-) = 1.05 \pm 0.02^{\text{stat}} \pm 0.15^{\text{syst}}$  was obtained. In the energy region  $3.5 \leq E_x \leq 7.2$  MeV the accuracy of our results deteriorates. The spectrum shows background contributions and, in addition, broad peaks containing contributions from several closely lying states are present. The value  $B(GT^-) = 1.59 \pm 0.02^{\text{stat}} \pm 0.38^{\text{syst}}$  was obtained for this region. We estimated the lower and upper limits for the strength contained in the GTGR, which was observed as a bump around 10 MeV. The obtained lower limit is around 8.4, while the upper limit is 11.2. This is only a rough estimation leading to a summed strength, in the  $0 \leq E_x \leq 17$  MeV energy region, of less than 55% of the Ikeda sum-rule-limit value. Contributions from the isovector spin giant dipole resonance (IVSGDR) and isovector spin giant monopole resonance (IVSGMR) also have to be considered, which further can lower the summed  $B(GT^-)$  value. However, these contributions are minor for the analyzed energy region of the spectrum corresponding to scattering angles between  $0^\circ$  and  $0.3^\circ$ , which

was used for extracting the  $B(GT)$  values; the IVSGDR has a minimum at these angles and the IVSGMR peaks at a much higher excitation energy.

The obtained  $B(GT^-)$  distribution was combined with the  $B(GT^+)$  distribution obtained in the study of the  $^{64}\text{Zn}(d, ^2\text{He})^{64}\text{Cu}$  reaction and the nuclear matrix element of the  $2\nu 2\beta$  from the gs of  $^{64}\text{Zn}$  to the gs of  $^{64}\text{Ni}$  was deduced [28].

These experimental results supplement the data base needed to calibrate theoretical models. The  $B(GT^-)$  distribution obtained in our study is an important benchmark for extending the presently existing residual interactions toward the heavy nuclei in the  $pf$  shell [28].

## ACKNOWLEDGMENTS

This experiment was performed at RCNP, Osaka University, under Experimental Program E210. The authors are grateful to the accelerator group of RCNP for providing a high quality  $^3\text{He}$  beam. The Ghent group acknowledges support from FWO-Flanders. L.P., T.A., and A.N. acknowledge support from the 21st Century COE program "Toward a New Basic Science" of the Graduate School of Science, Osaka University. Y.F. acknowledges support from Monbukagakusho, Japan, under Grant 18540270.

- 
- [1] Balraj Singh, Nucl. Data Sheets **108**, 197 (2007).  
 [2] T. N. Taddeucci *et al.*, Nucl. Phys. **A469**, 125 (1987).  
 [3] L. Popescu *et al.*, Phys. Rev. C **75**, 054312 (2007).  
 [4] F. Osterfeld, Rev. Mod. Phys. **64**, 491 (1992).  
 [5] E.-W. Grewe *et al.*, Phys. Rev. C **76**, 054307 (2007).  
 [6] A. Negret *et al.*, Phys. Rev. Lett. **97**, 062502 (2006).  
 [7] Y. Fujita *et al.*, J. Phys. G: Nucl. Part. Phys. **35**, 014041 (2008).  
 [8] K. Langanke and G. Martínez-Pinedo, Rev. Mod. Phys. **75**, 819 (2003).  
 [9] Y. Fujita *et al.*, Nucl. Phys. **A687**, 311 (2001).  
 [10] Y. Fujita, Nucl. Phys. **A805**, 408c (2008).  
 [11] J. Rapaport and E. Sugarbaker, Annu. Rev. Nucl. Part. Sci. **44**, 109 (1994).  
 [12] Y. Fujita *et al.*, Phys. Rev. C **59**, 90 (1999).  
 [13] Y. Fujita *et al.*, Phys. Rev. C **67**, 064312 (2003).  
 [14] Y. Fujita *et al.*, Phys. Rev. C **75**, 057305 (2007).  
 [15] T. Wakasa *et al.*, Nucl. Instrum. Methods A **482**, 79 (2002).  
 [16] M. Fujiwara *et al.*, Nucl. Instrum. Methods A **422**, 484 (1999).  
 [17] RCNP web-site, <http://www.rcnp.osaka-u.ac.jp>.  
 [18] T. Noro *et al.*, RCNP Annual Report, 177 (1991).  
 [19] Y. Fujita *et al.*, Nucl. Instrum. Methods B **126**, 274 (1997).  
 [20] H. Fujita *et al.*, Nucl. Instrum. Methods A **469**, 55 (2001).  
 [21] H. Fujita *et al.*, Phys. Rev. C **75**, 034310 (2007).  
 [22] Y. Fujita *et al.*, Phys. Rev. C **66**, 044313 (2002).  
 [23] L. Popescu *et al.*, J. Phys. G: Nucl. Part. Phys. **31**, S1945 (2005).  
 [24] K. Schreckenbach *et al.*, Phys. Lett. **B349**, 427 (1995).  
 [25] F. D. Becchetti, D. Dehnhard, and T. G. Dzubay, Nucl. Phys. **A168**, 151 (1971).  
 [26] J. Jänecke *et al.*, Phys. Rev. C **48**, 2828 (1993).  
 [27] T. Wakasa *et al.*, Phys. Rev. C **55**, 2909 (1997).  
 [28] E.-W. Grewe *et al.*, Phys. Rev. C **77**, 064303 (2008).  
 [29] K. Langanke *et al.*, Phys. Rev. Lett. **90**, 241102 (2003).  
 [30] T. Adachi *et al.*, Nucl. Phys. **A788**, 70 (2007).